

CLUE-MARK: Watermarking Diffusion Models using CLWE

Kareem Shehata, Aashish Kolluri, and Prateek Saxena
School of Computing, National University of Singapore
 {kareem, aashish7, prateeks}@comp.nus.edu.sg

Abstract—As AI-generated images become widespread, reliable watermarking is essential for content verification, copyright enforcement, and combating disinformation. Existing techniques rely on heuristic approaches and lack formal guarantees of undetectability, making them vulnerable to steganographic attacks that can expose or erase the watermark. Additionally, these techniques often degrade output quality by introducing perceptible changes, which is not only undesirable but an important barrier to adoption in practice.

In this work, we introduce CLUE-MARK, the first provably undetectable watermarking scheme for diffusion models. CLUE-MARK requires no changes to the model being watermarked, is computationally efficient, and because it is provably undetectable is guaranteed to have no impact on model output quality. Our approach leverages the Continuous Learning With Errors (CLWE) problem — a cryptographically hard lattice problem — to embed watermarks in the latent noise vectors used by diffusion models. By proving undetectability via reduction from a cryptographically hard problem we ensure not only that the watermark is imperceptible to human observers or adhoc heuristics, but to *any* efficient detector that does not have the secret key. CLUE-MARK allows multiple keys to be embedded, enabling traceability of images to specific users without altering model parameters. Empirical evaluations on state-of-the-art diffusion models confirm that CLUE-MARK achieves high recoverability, preserves image quality, and is robust to minor perturbations such as JPEG compression and brightness adjustments. Uniquely, CLUE-MARK cannot be detected nor removed by recent steganographic attacks.

1. Introduction

In an era where AI-generated images are becoming increasingly common, identifying whether an image originates from a model is critical for combating disinformation and settling copyright claims. Watermarking, wherein a signal is inserted into an image such that it can later be recovered, has emerged as an essential tool to determine the provenance of images. Current approaches to watermarking AI-generated images remain ad-hoc. For example, TREE RING [1] was conjectured to be undetectable and robust, but no proof as such was given. While an important step forward, TREE RING watermarks can be both detected and removed by standard steganalysis [2], i.e. averaging the difference between watermarked and non-watermarked images.

This is more than a security concern; it shows that the watermark affects the output of the model such that the output images are both quantitatively and qualitatively different from the original. After spending considerable effort to train and optimise large diffusion models, providers and users are understandably reluctant to then degrade the quality of the images they generate in order to watermark them.

Thus for both security and quality reasons, it is important that the watermark be *provably undetectable*, by which we mean that a watermarked image be indistinguishable from an unwatermarked image. A rigorous reduction from a cryptographically hard problem is needed, otherwise it may turn out that a watermark that was conjectured to be undetectable is in fact detectable by some other means, or may affect downstream applications. By proving undetectability, we ensure that the watermark does not compromise the quality of the generated images and remains stealthy to detectors.

In this work we will show how cryptographic techniques can be used to inject a watermark into diffusion model generated images such the watermark is provably indistinguishable from the no watermark case. Previous work on watermarking AI-generated images has shown that by injecting signals into the noise inputs of diffusion models, it is possible to recover watermarks even after significant modifications to the image by inverting the model and analyzing the noise for the watermark signal [1], [3]. While these techniques demonstrated robustness to perturbations arising in benign applications, they were not provably undetectable and more recent work has shown that they can be detected and removed by steganalysis [2].

Undetectability from CLWE. Our approach is to modify the noise input to a diffusion model using a distribution based on the Continuous Learning With Errors (CLWE) problem [4]. The intuitive idea is that this distribution produces samples that appear normal in all directions except for a secret direction in which it has a signature pattern that is different from normal. By carefully constructing the watermark, we can prove that any process that can reliably detect the watermark can be used to distinguish a CLWE distribution from a normal distribution. This problem is known to be cryptographically hard [4], and thus we can be confident that CLUE-MARK is undetectable for *any* downstream process, not just those we have tested, ensuring image quality and undetectability. Moreover, because CLUE-MARK only modifies the input noise, it does not modify the model in any way and does not require

retraining. Meanwhile, if the secret direction is known then the watermark can be efficiently recovered by inverting the model and checking for the signature.

A secondary advantage to this approach is that it supports multiple keys, and several keys can be used in a single watermark. For example, a provider may have a key for all images generated by a model and a key for each user, allowing them to quickly check if an image came from the model before checking which user generated it.

In an ideal world, the perfect scheme would be such that watermarked images can always be verified to contain the watermark (completeness) and unmarked images can always be verified to not contain the watermark (soundness), without degrading image quality, and despite perturbations to the image that do not degrade image quality. Unfortunately, we prove in Section 4 that such perfect watermarking is impossible theoretically. As such, we must choose which properties are most important for our application. In this work we aim first for undetectability that can be rigorously proven, and then secondarily for a watermark that is as robust as possible.

Empirical Results. While CLUE-MARK is theoretically undetectable, the question becomes whether it is usable in practice. Image sampling and inversion of diffusion models adds considerable noise, and thus the watermark may not be recoverable. If so, can the watermark be recovered after applying common perturbations? To that end, we evaluate CLUE-MARK on commonly used diffusion models and datasets to verify undetectability, recoverability, image quality, and robustness. We show that CLUE-MARK is indeed undetectable by common means, produces images with the same quality as the original, and is recoverable with the secret key. We also show that it is robust to small perturbations, such as JPEG compression and brightness.

Contributions. Our contribution is a novel and practical watermarking scheme, CLUE-MARK, for images generated by modern diffusion AI models. It is provably undetectable, in the sense that detectability is as hard as distinguishing the CLWE distribution from a Gaussian—a standard cryptographic hardness assumption in lattice-based cryptography.

2. Motivation and Problem Setup

Diffusion models, such as Stable Diffusion [5], [6], have quickly emerged as the go-to AI models for generating very high quality and customizable images. They have been adopted across diverse fields such as digital art and content creation, e-commerce, and aiding research in natural sciences (see survey [7]). The process to generate an image from a diffusion model is called “sampling”, in which the model is given a text embedding and a noise vector (in the latent space of the model, hence this is often called the “latent vector” or “latent noise”), and the model iteratively removes the noise to produce an image described by the text embedding, as illustrated in Figure 1. We refer to [5],

[6] for understanding the details of diffusion models, and describe only the parts that are necessary for our work.

Definition 2.1 (Diffusion Model Sampling). The process to sample a diffusion model is defined as the function:

$$\text{Sample}_\theta(\pi \in \mathcal{T}^*; \mathbf{z} \in \mathbb{R}^n) \rightarrow \mathbf{x} \in \mathbb{R}^N$$

where θ is the model parameters, π is the embedding of the text prompt, \mathbf{z} is the noise vector, and \mathbf{x} is the generated image. The noise vector is drawn from a standard normal (Gaussian) distribution, that is $\mathbf{z} \sim \mathcal{N}(\mathbf{0}, \mathbf{I})$.

Watermarking Diffusion Models. Malicious actors can (and do) misuse diffusion models to create realistic fake images, like deepfakes, which pose serious risks. They use these images to blackmail [8], execute scams [9], spread disinformation [10], and manipulating individuals with potentially harmful financial, social, and political consequences. Watermarking is a proposed measure to detect AI-generated content. Model developers, such as OpenAI and Google, have pledged to watermark the content they generate with active monitoring and government oversight [11], [12], [13].

Watermarking an image refers to implanting a signal within it such that the signal can later be recovered. If an image can be confirmed to contain the watermark signal, this offers proof of the provenance of the image. In a secret key scheme, only those with the key can verify an image’s origin. Consider a company that hosts a closed-source model. If the company watermarks the images generated by the model using a secret key, they can later verify whether an image was generated by the model by checking for the watermark using the key. They can also give the key to another entity to do verification, for example a social media platform that wants to verify the authenticity of images uploaded by users. The company may also assign a key to each user in order to trace which user was responsible for generating a particular image. Watermarks may be applied to images after generation (“post-process”) or during model execution (“in-process”). Diffusion models offer another option: watermarking the noise vector \mathbf{z} used to generate the image (“pre-process”), as introduced by Tree Rings [1]. In this work we focus on secret-key pre-process watermarking. See Figure 2 for an illustration of the use cases.

Problem. Despite the potential benefits of watermarking AI generated images, adoption has been limited [14]. One reason for this is image quality. Large models that generate high-quality images are expensive to train and serve, and both companies and users are sensitive to any degradation in image quality. Further, changes to image quality may also affect the performance of downstream tasks. For example, if the generated images are used to train another model or as inputs to a larger process, any changes in the images may affect the performance of the system as a whole.

Existing watermarking techniques for diffusion models have a noticeable impact on the images generated. Post-processing techniques, e.g. embedding a signal into the output pixel data and even AI-based techniques, have visible

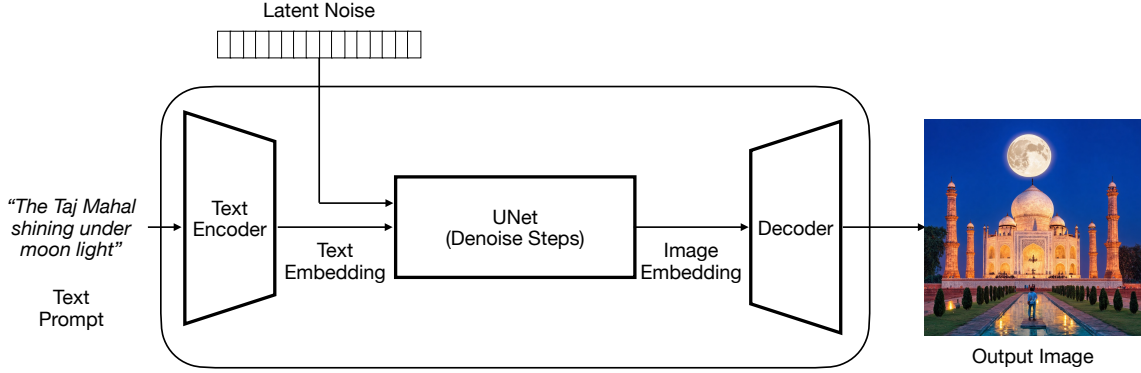


Figure 1: Sampling images from latent diffusion models



Figure 2: Watermarking Use Cases.

quality losses [1]. As we evaluate in this work, state-of-the-art techniques such as TREE RING and GAUSSIAN SHADING, despite aiming for not being perceptible, produce images with a significant quality differences from their unwatermarked equivalents (see Section 6.4). This is because of ad-hoc design choices and the lack of provable guarantees. When evaluated over a large set of images, it can be seen that the watermarked images are biased (less diverse statistically) than the unwatermarked images. Further, recent attacks have shown that the watermarks can be detected, removed, and forged using standard steganographic techniques [2].

2.1. Undetectable Watermarking

In this work, we aim to solve this problem by designing *provably undetectable* watermarking. By this we mean that distinguishing between watermarked and unwatermarked images must be computationally at least as hard as solving a cryptographic problem. This ensures that there is a negligible difference between watermarked and unwatermarked images for *any* downstream application. Even a determined adversary trying just to detect the presence of a watermark faces a challenge at least as hard as breaking state-of-the-art cryptography. This approach embodies a secure by construction principle, in contrast to existing techniques which empirically evaluate against specific attacks but cannot rule out the existence of other effective attacks. In order to construct a provable scheme, we first formally define the watermarking process.

Definition 2.2 (Watermarking). A watermarking function is defined as the tuple of functions (Setup, Mark, Extract):

$$\begin{aligned} \text{Setup}_\theta(1^\lambda) &\rightarrow k \in \mathcal{K} \\ \text{Mark}_\theta(\pi \in \mathcal{T}^*; k \in \mathcal{K}) &\rightarrow \mathbf{x} \in \mathbb{R}^N \\ \text{Extract}_\theta(\mathbf{x} \in \mathbb{R}^N; k \in \mathcal{K}) &\rightarrow \{0, 1\} \end{aligned}$$

where λ is a security parameter, θ is the model parameters, π is the embedding of the text prompt, k is the secret key, and \mathbf{x} is the generated image.

In order to be useful, we require that a watermarking scheme be at least complete and sound, for which we use Definitions 2.3 and 2.4.

Definition 2.3 (Watermark Completeness). A watermarking scheme (Setup, Mark, Extract) is δ -complete if for all $\pi \in \mathcal{T}^*$:

$$\Pr[\text{Extract}_\theta(\text{Mark}_\theta(\pi; k); k) = 1 | k \leftarrow \text{Setup}_\theta(1^\lambda)] \geq 1 - \delta$$

Definition 2.4 (Watermark Soundness). A watermarking scheme (Setup, Mark, Extract) is δ -sound if for all $\pi \in \mathcal{T}^*$:

$$\begin{aligned} \Pr[\text{Extract}_\theta(\text{Sample}_\theta(\mathbf{z}; \pi); k) = 1] \\ k \leftarrow \text{Setup}_\theta(1^\lambda), \mathbf{z} \leftarrow \mathcal{N}(\mathbf{0}, \mathbf{I}) \leq \delta \end{aligned}$$

Before we can define undetectability, we must define formally what we mean by “distinguishing” and how we measure success. For this we use Definition 2.5.

Definition 2.5 (Advantage of a Distinguisher). Let $D^{\mathcal{O}} \rightarrow \{0, 1\}$ be a distinguisher with access to oracle \mathcal{O} . Define the advantage of D in distinguishing \mathcal{O}_1 and \mathcal{O}_2 as:

$$Adv_{D, \mathcal{O}_1, \mathcal{O}_2} = |\Pr [D^{\mathcal{O}_1}(1^\lambda) = 1] - \Pr [D^{\mathcal{O}_2}(1^\lambda) = 1]|$$

We want to ensure that our watermarking scheme is *undetectable*, that is, that the output of the watermarking process is indistinguishable from non-watermarked images generated by the model. We formally define this in Definition 2.6.

Definition 2.6 (Provable Undetectability). Let \mathcal{M}_θ be an oracle that on input $\pi \in \mathcal{T}^*$ samples $\mathbf{z} \leftarrow \mathcal{N}(\mathbf{0}, \mathbf{I})$ and returns $\text{Sample}_\theta(\pi; \mathbf{z})$. Let $\mathcal{W}_{\theta, k}$ be an oracle that on input $\pi \in \mathcal{T}^*$ returns $\text{Mark}_\theta(\pi; k)$ for a fixed key $k \leftarrow \text{Setup}_\theta(1^\lambda)$. A watermarking scheme (Setup, Mark, Extract) is undetectable if for all *probabilistic polynomial-time* PPT distinguishers D , $Adv_{D, \mathcal{M}_\theta, \mathcal{W}_{\theta, k}} \leq \text{negl}(\lambda)$.

3. The CLUE-MARK Approach

Our approach to watermarking images is based on the idea of modifying the latent noise vector of a diffusion model (i.e. pre-process watermarking). Recall that a diffusion model takes as input a latent vector that is expected to be from the standard gaussian distribution. In our approach, we instead use a latent vector that is drawn from the hCLWE distribution (which will be defined in Section 3.1). This vector is indistinguishable from the standard gaussian distribution to all PPT-computable functions without the secret key, but can be efficiently distinguished when the secret key is known. We call using hCLWE samples to generate an image the *watermark injection* process. To test whether an image is watermarked, a system with access to the secret key uses the *watermark recovery* process. During recovery, we invert the diffusion model to get an estimate of the initial latent vector from the watermarked image. We then use the secret key to determine if the latent vector is from the hCLWE distribution, and if so, then it is very likely that the image is watermarked using that key.

In this section we describe the high-level approach of watermarking, including the necessary background on CLWE, and the watermark injection and recovery processes. We will prove undetectability of the construction in Section 4.

3.1. Background on CLWE

Consider the scatter plot shown in Figure 3. If you were to look at the distribution of the points along either axis, it would look like a standard gaussian distribution. But if you were to plot the points along the line $y = -x$, you would notice that the points are periodic. That is, that they're bunched together around $-1, -1/2, 0, 1/2, 1$, and so on. In two dimensions you can see this immediately by looking at the scatter plot, but what if the points are in three dimensions? The points would form a sphere from nearly any angle you look at, except if you found the “secret

direction” you would notice the the points form slices and are again periodic¹.

This is the essence of the homogenous Continuous Learning With Errors (hCLWE) problem². Intuitively, it becomes harder to find the secret direction as you increase the number of dimensions, as the number of directions you have to check grows exponentially. Deciding whether a set of points (from now on let us call them samples) are normally distributed in all directions, or if there is a secret direction in which they are periodic has been proven to be as hard as solving worst-case lattice problems [4].

To write this more formally, consider a unit vector $\mathbf{w} \in \mathbb{R}^n$ chosen uniformly at random, and a set of samples $\mathbf{y}_1, \dots, \mathbf{y}_m \in \mathbb{R}^n$ that are drawn from a standard gaussian distribution in all directions except for the direction \mathbf{w} , in which case the distribution is shown in Figure 4. This produces the well-known “gaussian-pancakes” distribution, which produces periodic slices with separation $\approx 1/\gamma$ and width $\approx \beta/\gamma$ in the secret direction \mathbf{w} , and standard gaussian in all others. The hCLWE problem is to determine the secret direction \mathbf{w} given a polynomial number of samples $\{\mathbf{y}_i\}_{i \in [m]}$. The decision variant of hCLWE is to distinguish between samples from the hCLWE distribution and from the standard multivariate normal. This leads to Theorem 1, an informal statement of the CLWE hardness theorem; see [4] for the more formal statement, proof, and further details.

Theorem 1 (hCLWE Hardness Informal). *For $\gamma = \Omega(\sqrt{n}), \beta \in (0, 1)$ such that β/γ is polynomially bounded, if there exists an algorithm that can efficiently distinguish the $hCLWE_{\gamma, \beta}$ distribution from the standard multivariate gaussian distribution, then there exists an efficient algorithm that approximates worst-case lattice problems to within a factor polynomial in n .*

Such lattice problems are considered cryptographically hard for appropriately chosen parameters γ and β . Assuming that no PPT algorithm can solve them, then we can state that no PPT algorithm can solve the decision hCLWE problem non-negligible probability.

3.2. Watermarks from CLWE

Blocking. The hCLWE distribution assumes a number of high-dimensional samples, while the noise vector required for the initial diffusion model latents is a single vector. The solution is to divide the latent vector into a number of non-overlapping blocks, each of which is treated as a sample from the hCLWE distribution. The blocks must each be large enough to ensure undetectability, but small enough to ensure enough samples to recover the watermark even if some blocks are lost or corrupted by noise. As we will see in Section 6.1, for a latent vector of dimensions $4 \times 64 \times 64$ we choose a block size of either $4 \times 1 \times 1$ or $4 \times 4 \times 4$

1. The original CLWE presentation at <https://youtu.be/9CB4KcoRB9U?t=60> has an animation that illustrates this effect clearly.

2. Homogenous CLWE is a special case of the more general CLWE problem.

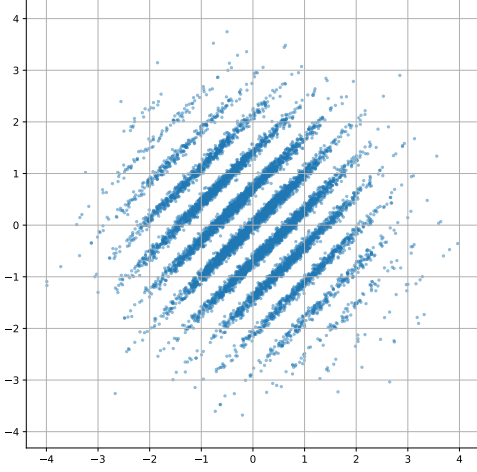


Figure 3: Example scatter plot of 10,000 samples from the hCLWE distribution with secret direction $(1/\sqrt{2}, -1/\sqrt{2})$, $\gamma = 2, \beta = 0.1$.

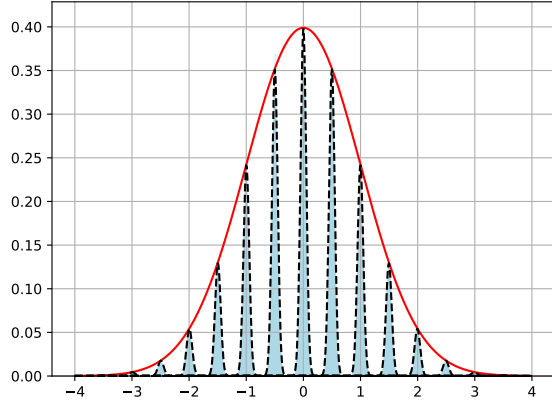


Figure 4: The hCLWE PDF with $\gamma = 2, \beta = 0.1$ in the secret direction compared with the standard gaussian distribution.

for our watermark evaluations, but for the moment we leave this as an implementation parameter.

Frequency Domain. In order to improve robustness to perturbations, we use a standard technique in image watermarking (see [15]): we apply the hCLWE samples in the frequency domain of the latents. That is we take the inverse discrete wavelet transform (IDWT) of the hCLWE samples to arrive at the latent vector used to generate the image. The process for image generation is shown in Figure 5. The watermark recovery process reverses this process, but requires additional steps in order to extract the watermark in the presence of noise and perturbations.

Recovery. We now have an approach that allows us to embed an hCLWE distribution in the latent space of a diffusion model, which we then use to produce an image. The question becomes: how do we determine if an image contains a watermark? From recent work [16], [17], we can invert the diffusion model to get an estimate of the original latent vector (assuming the image is not perturbed). Dividing the latent vector into blocks is then trivial, but the resulting blocks are subject to noise and perturbation. Given these noisy blocks and the secret direction of the hCLWE distribution, how do we determine if the watermark is present?

First, we can measure the error from the ideal hCLWE distribution by computing the inner product with the secret direction to get a set of z_i values:

$$z_i = \gamma \langle \mathbf{y}_i, \mathbf{w} \rangle \pmod 1$$

In the no-watermark case, we expect that for well-chosen parameters the z_i values will be uniformly distributed in $[0, 1)$. In the watermark case, we expect that the z_i values will be concentrated near zero, with the strength of the concentration depending on β , noise, and perturbations. This produces the situation shown in Figure 7, which shows the result of a statistical simulation comparing z_i values calculated from samples drawn from a standard normal, hCLWE, and hCLWE with noise from a normal distribution of width 0.2.

Thus our problem boils down to distinguishing two distributions. There are many well-known distinguishing techniques one can use; we use the standard Kolmogorov-Smirnov (KS) statistic in this work. Intuitively, the KS statistic gives a measure of the difference between a set of samples from a reference distribution, with a higher score indicating that the samples are less likely to have been drawn that distribution. In our case we use the uniform distribution as the null hypothesis, and use KS to measure the distance of the given z_i values from the uniform distribution. If the KS statistic is above a certain threshold, then we can reject the null hypothesis and say that the samples are not gaussian in the secret direction, and therefore the watermark is present.

In concrete terms, the KS statistic is the maximum distance between the empirical CDF of the samples and the expected CDF of the reference distribution. As illustrated in Figure 8, in the statistical simulation, the KS statistic for the standard normal samples is 0.036, indicating a very small deviation from uniform, while the KS statistic for the hCLWE samples with $\beta = 0.1$ is 0.774 indicating a large deviation from uniform. Finally, the hCLWE samples with gaussian noise of variance 0.2 produces a KS statistic of 0.575, indicating a strong presence of the watermark despite the noise. Thus, using KS we get a strong indication of the presence of the watermark despite significant noise.

The resulting recovery process is shown in Figure 6. In terms of parameters, we set n (the number of dimensions per CLWE sample), γ and β (CLWE parameters) for security of the reductions in Section 6.1, and m follows from the size of the latent space.

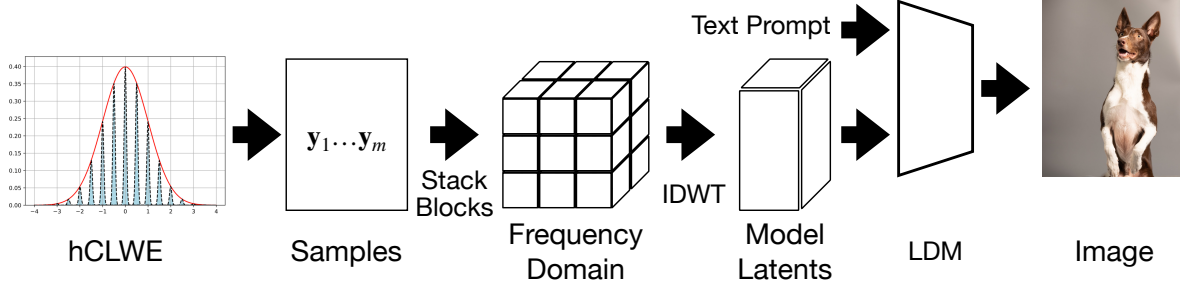


Figure 5: CLUE-MARK watermark injection process.

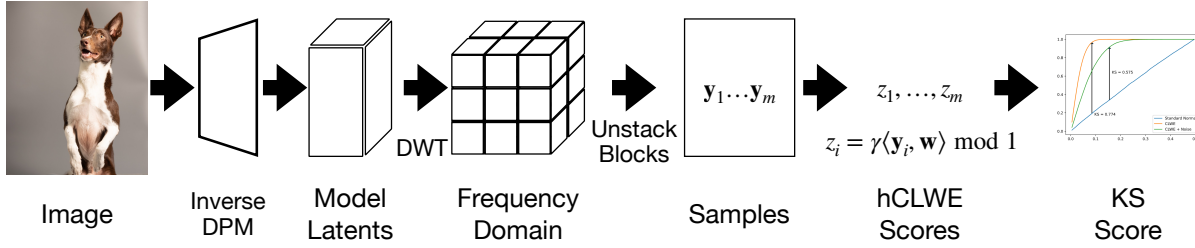


Figure 6: Watermark recovery process.

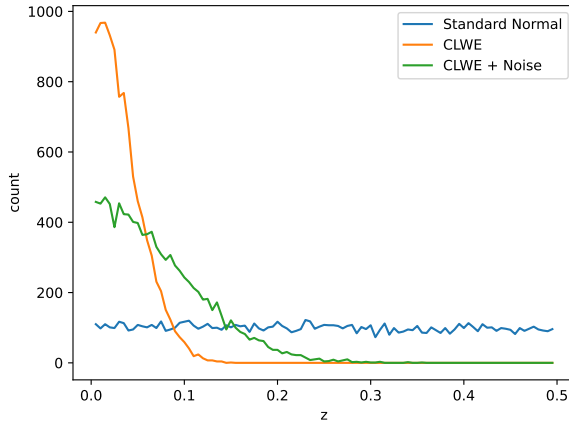


Figure 7: Histogram of $|z_i|$ values from statistical simulation of 10,000 samples.

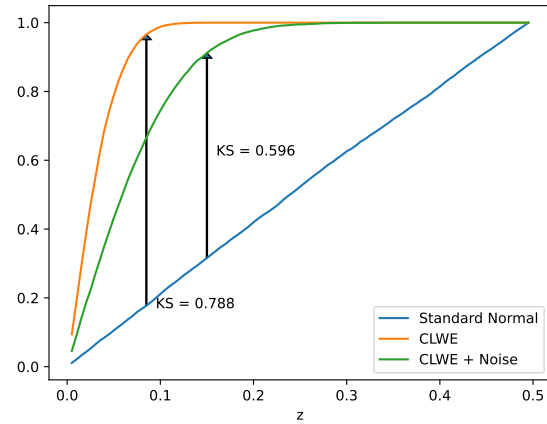


Figure 8: Empirical CDF of CLWE errors from a statistical simulation of 10,000 points drawn from several distributions.

4. Security Proof

In this section, we provide the formal definitions and proofs of completeness, soundness, and undetectability of CLUE-MARK.

4.1. Formal Definitions

Define:

$$\rho_s(\mathbf{x}) = \exp(-\pi\|\mathbf{x}/s\|^2) \quad (1)$$

Where $\mathbf{x} \in \mathbb{R}^n$. Note that $\rho_s(\mathbf{x})/s^n$ is the PDF of the gaussian distribution with covariance $s^2/2\pi \cdot I_n$.

Definition 4.1 (hCLWE Distribution). Let $\mathbf{w} \in \mathbb{R}^n$ be a unit vector, and $\beta, \gamma > 0$ be parameters. Define the homogeneous continuous learning with errors (hCLWE) distribution $H_{\mathbf{w},\beta,\gamma}$ over \mathbb{R}^n to have density at point \mathbf{y} proportional to:

$$\rho(\mathbf{y}) \cdot \sum_{k \in \mathbb{Z}} \rho_\beta(k - \gamma\langle \mathbf{w}, \mathbf{y} \rangle)$$

Definition 4.2 (Decision hCLWE Problem). Let $\mathbf{w} \in \mathbb{R}^n$ be a unit vector drawn uniformly at random, and $\beta, \gamma > 0$ be parameters. Let \mathcal{N} be an oracle that responds to queries with samples from $\mathcal{N}(0, I_n)$, and let $\mathcal{H}_{\mathbf{w}, \beta, \gamma}$ be an oracle that responds with samples from $H_{\mathbf{w}, \beta, \gamma}$. The decision hCLWE problem is to distinguish \mathcal{N} and $\mathcal{H}_{\mathbf{w}, \beta, \gamma}$. That is for distinguisher D , we say that D solves the decision hCLWE problem with advantage $Adv_{D, \mathcal{N}, \mathcal{H}_{\mathbf{w}, \beta, \gamma}}$.

Assumption 1.1 (hCLWE). No PPT distinguisher D can solve the decision hCLWE problem with non-negligible advantage.

4.2. Undetectability

Theorem 2 gives our main theoretical result: detecting the watermark is as hard as solving the decision hCLWE problem. Before we dive into the technical details of the proof, we first provide an intuitive explanation. Our proof is by reduction, that is if there exists a distinguisher that can reliably distinguish watermarked and unwatermarked images, then we can use that distinguisher to solve the decision hCLWE problem. Recall that in the hCLWE problem the distinguisher is given an oracle that for all queries returns samples from either the hCLWE distribution or the standard normal distribution. In the reduction, whenever the watermark distinguisher requests an image, we construct the latent vector from samples from the given oracle, which we give to the latent diffusion model to generate an image, before passing the image back to the watermark distinguisher. If the oracle gives us standard normal samples, then this corresponds to the unwatermarked case, while if the oracle gives us hCLWE samples, then this corresponds to the watermarked case. Other than the samples used to build the initial latent vector, the process is identical and thus the difference in probability between the two cases can only come from the samples. Note that if the latent vector has dimension mn , then each image generated requires m samples from the oracle. If the watermark distinguisher has a non-negligible advantage, then so does our hCLWE distinguisher.

Theorem 2. Assuming the hCLWE assumption holds for n dimensions with parameters γ, β , the CLUE-MARK watermarking scheme described in Section 3 with latent vectors of dimension mn such that m is at most polynomial in n is undetectable by Definition 2.6.

Proof. Consider a PPT distinguisher $D^\mathcal{O}$ that has non-negligible advantage ϵ in distinguishing between watermarked and non-watermarked images, that is $Adv_{D, \mathcal{M}_\theta, \mathcal{W}_{\theta, k}} \geq \epsilon$.

We now construct D' that solves the decision hCLWE problem, given access to \mathcal{O}' , which is either \mathcal{N} , an oracle that returns samples from the standard normal, or $\mathcal{H}_{\mathbf{w}, \beta, \gamma}$, an oracle that gives samples from the hCLWE distribution³.

3. The oracle is consistent for all queries, that is if the oracle is \mathcal{N} then all results are standard normal. The oracle does change distributions between queries.

Algorithm 1: Method to convert samples from a base distribution to hCLWE.

Input: Secret direction \mathbf{w} , Samples

$\mathbf{y}_1, \dots, \mathbf{y}_m \in \mathbb{R}^n$

Output: Samples $\mathbf{y}'_1, \dots, \mathbf{y}'_m \in \mathbb{R}^n$

```

1  $\gamma' \leftarrow \sqrt{\beta^2 + \gamma^2}$ ;
2 for  $i \in [m]$  do
3    $k_i \leftarrow \lceil \gamma' \langle \mathbf{y}_i, \mathbf{w} \rangle \rceil$ ;
4    $z_i \leftarrow \mathcal{N}(0, \beta)$ ;
5    $\mathbf{y}'_i \leftarrow \mathbf{y}_i + ((z_i + k_i \cdot \gamma / \gamma') / \gamma' - \langle \mathbf{y}_i, \mathbf{w} \rangle) \mathbf{w}$ ;
6 return  $\mathbf{y}'_1, \dots, \mathbf{y}'_m$ 

```

Distinguisher D' works as follows:

- 1) On receiving a request to \mathcal{O} with query π , D' :
 - a) requests m samples from the oracle, $\mathbf{y}_1, \dots, \mathbf{y}_m \leftarrow \mathcal{O}'$, $\mathbf{y}_i \in \mathbb{R}^n$, where mn is the size of the latent space of the model.
 - b) Assembles the samples to form the dimensions of the latent space, i.e. $\mathbf{z}' \leftarrow (\mathbf{y}_1, \dots, \mathbf{y}_m) \in \mathbb{R}^{mn}$.
 - c) Applies the inverse DWT to the assembled samples to obtain a latent vector, i.e. $\mathbf{z} \leftarrow \text{IDWT}(\mathbf{z}')$.
 - d) Uses the result as the latent vector to sample an image from the model, $\mathbf{x} \leftarrow \text{Sample}_\theta(\pi, \mathbf{z})$.
 - e) Forwards the image \mathbf{x} to D .
- 2) D' outputs the same result as D .

Clearly, if D has advantage ϵ in distinguishing watermarked and unwatermarked images, then D' has at least ϵ advantage in distinguishing hCLWE samples from standard normal samples. Since all of the operations in D' are polynomial time, this contradicts the hCLWE assumption. \square

4.3. Sampling from hCLWE

Sampling from the hCLWE distribution is non-trivial. In [4] it is suggested that the hCLWE distribution be sampled by rejection-sampling from the standard normal distribution. However, this is not practical for our setup, as not only does this require drawing many more samples than needed, it also assumes the base distribution is the standard normal and easy to sample. In our case, the base distribution is the model's latent space after a DWT transform. Rather than rejection sampling in this space, we propose a much simpler approach: beginning with samples of the appropriate base distribution (e.g. standard normal and then apply DWT), project the samples to the nearest CLWE point and then add noise in the secret direction. We can then reverse any transforms needed to get the samples in the required domain.

Algorithm 1 shows the details of this method, which is slightly more complicated due to the fact that the gaussian mixtures have width $\beta/\gamma' = \beta/\sqrt{\beta^2 + \gamma^2}$ and are separated by γ/γ'^2 . If $\beta \ll \gamma$ then $\gamma' \approx \gamma$ and this simplifies to the expected steps. Indeed, for practical purposes the difference is insignificant. This can be seen in Figure 4, as the blue

area is a histogram generated by a simulation of 10,000 samples using this approximation and is not simply the area under the dashed line (the expected PDF).

Claim 2.1. *The method shown in Algorithm 1, on input from the standard normal \mathcal{N} , produces samples from $H_{\mathbf{w},\beta,\gamma}$.*

Proof. Consider a single input sample y drawn from the standard normal \mathcal{N} . Let $\gamma' = \sqrt{\beta^2 + \gamma^2}$, $\tilde{y} = \langle \mathbf{y}, \mathbf{w} \rangle$ and $\mathbf{y}^\perp = \mathbf{y} - \tilde{y} \cdot \mathbf{w}$, i.e. \tilde{y} is the projection of \mathbf{y} in the secret direction and \mathbf{y}^\perp is the component of \mathbf{y} perpendicular to it. Set $k = \lceil \gamma' \tilde{y} \rceil$. We can now rewrite the output of the algorithm as:

$$\mathbf{y}' = \mathbf{y}^\perp + \left(\frac{z + k \cdot \gamma / \gamma'}{\gamma'} \right) \mathbf{w} = \mathbf{y}^\perp + \tilde{y}' \mathbf{w}$$

From this we can write the PDF of \mathbf{y}' as the convolution of the choices of k and z :

$$\rho(\mathbf{y}^\perp) \cdot \sum_{z \in \mathbb{Z}} \rho_{\gamma'}(k) \rho_\beta(z)$$

By substituting out z , we get:

$$\rho(\mathbf{y}^\perp) \cdot \sum_{z \in \mathbb{Z}} \rho_{\gamma'}(k) \rho_{\beta/\gamma'}(\tilde{y}' - k\gamma/\gamma'^2)$$

This expression can be manipulated algebraically to achieve the same expression as in Definition 4.1. \square

5. Are Perfect Watermarks possible?

Ideally, a watermark should be robust in the sense that perturbations that do not affect the image quality should not remove the watermark. Unfortunately, it is impossible for a watermark to simultaneously satisfy completeness, soundness, provable undetectability, and perfect robustness. We formalize the statement and provide a proof.

Undetectability. Recall that in Definition 2.6 we defined undetectability as the property that no PPT algorithm can distinguish between a watermarked image and its unwatermarked counterpart, without access to the watermarking key k . In other words, the *quality* of the distribution of the images before and after watermarking does not change, from the perspective of any *quality oracle that does not have access to keys and is computationally bounded*. Lemma 2.1 bounds the distance between distributions observed under two keys k, k' against any such quality oracle. Informally, this tells us that the quality of images generated from watermarking, even with different keys, is the same to any downstream function without the watermarking keys.

Lemma 2.1. *For an undetectable watermarking scheme, no PPT distinguisher D can distinguish between $\mathcal{W}_{\theta,k}$ and $\mathcal{W}_{\theta,k'}$ with non-negligible advantage. That is, $Adv_{D,\mathcal{W}_{\theta,k},\mathcal{W}_{\theta,k'}} \leq negl(\lambda)$, assuming D has no access to the keys k or k' .*

Proof. The proof is by a standard hybrid argument. Consider any PPT distinguisher D . From the definition of undetectability, we have that $Adv_{D,\mathcal{M}_\theta,\mathcal{W}_{\theta,k}} \leq negl(\lambda)$ and $Adv_{D,\mathcal{M}_\theta,\mathcal{W}_{\theta,k'}} \leq negl(\lambda)$. By the triangle inequality:

$$\begin{aligned} Adv_{D,\mathcal{W}_{\theta,k},\mathcal{W}_{\theta,k'}} &\leq Adv_{D,\mathcal{M}_\theta,\mathcal{W}_{\theta,k}} + Adv_{D,\mathcal{M}_\theta,\mathcal{W}_{\theta,k'}} \\ &\leq 2 \cdot negl(\lambda) = negl(\lambda). \end{aligned}$$

\square

Perfect Robustness. If we allow arbitrary perturbations of the image, it is trivial to remove the watermark by simply replacing the image with another completely different image. What may not be immediately apparent is that even if we restrict to perturbations that maintain image quality, it is still impossible to have a watermark that is robust to such perturbations and is undetectable. Here we define quality in the same way as undetectability: the quality of two sets of images is the same if no PPT algorithm can distinguish the distributions with non-negligible advantage.

A watermarking scheme is perfectly robust if a watermarked image, after perturbations that do not change its quality, is treated the same as the unperturbed image by the (keyed) verifier, i.e., the *Extract* function accepts the perturbed image if the watermarked image before perturbation was accepted. More formally, a *perfectly robust watermark* is one wherein given an $x \leftarrow \text{Mark}(k, \pi)$, no PPT adversary can find an image x' of the same quality as x but for which $\text{Extract}(k, x) \neq \text{Extract}(k, x')$.

Theorem 3. *No watermarking scheme satisfying soundness, completeness, undetectability, and perfect robustness exists.*

Proof. Assume for the sake of contradiction that a watermarking scheme satisfying all four properties exists. We can instantiate the scheme with a key $k \leftarrow \text{Setup}(1^\lambda)$ and by computing $x \leftarrow \text{Mark}(k, \pi)$ for an input π . By the *completeness* property, the *Extract*(k, x) must accept. Now consider the following generic attack strategy: The adversary who does not know k generates a fresh key $k' \leftarrow \text{Setup}(1^\lambda)$ and generates $x' \leftarrow \text{Mark}(k', \pi)$. Note that by Lemma 2.1, PPT algorithms without access to k and k' cannot distinguish the distributions of x and x' with non-negligible probability. Thus, x and x' have the same quality. We analyze the behavior of the original verifier, i.e., the distribution of the random variable *Extract*(k, x'):

- If the verifier *Extract*(k, x') accepts with probability more than $negl(\lambda)$, then it violates *soundness*. This is because $k' \neq k$ with high probability $1 - negl(\lambda)$, and with that probability, we have a PPT adversary who does not know k but has found x' that is accepted by the verifier with the key k .
- If the verifier *Extract*(k, x') rejects with probability more than $negl(\lambda)$, then the scheme violates *perfect robustness*—the adversary has efficiently⁴ found x' of

4. The adversary breaks the hardness criterion while sticking to the constraint stated for perfect robustness, i.e., knowing k' but not k .

same quality⁵ as x (by Lemma 2.1) without knowing k , and yet we have $Extract(k, x') \neq Extract(k, x)$.

We have derived a contradiction to the assumptions in both cases above, which are exhaustive and mutually exclusive. Thus, no watermarking scheme satisfies all 4 properties. \square

The attack strategy underlying our proof of Theorem 3 is realizable within practical threat models, such as those assumed in recent attacks on LLM watermarking schemes [18].

6. Evaluation

We answer the following questions in our evaluation.

RQ1: What practical CLWE parameters should be used for CLUE-MARK?

RQ2: How well can we recover the CLUE-MARK watermark after inverting the raw images?

RQ3: What is the quality of the images generated by CLUE-MARK?

RQ4: Do steganographic attacks work against CLUE-MARK?

RQ5: How robust is CLUE-MARK to benign transformations, such as JPEG compression, on the watermarked images?

6.1. RQ1. Practical Parameters

The CLWE problem is relatively recent candidate for a cryptographic hardness assumption, and as such, optimal parameters for security are not fully settled. The original reductions from hard problems to CLWE [4] require that $\gamma \geq 2\sqrt{n}$ and a non-trivial value of $\beta > 0$, using a quantum reduction. In [19], it is further confirmed using a classical reduction that $\gamma = \tilde{\Omega}(\sqrt{n})$ is required for theoretical security. This suggests that a natural design choice for embedding a CLWE distribution in a latent space of $4 \times 64 \times 64$ floating point numbers that are normally distributed is to divide the space into $n = 4 \times 1 \times 1$ blocks, and set $\gamma = 2\sqrt{4} = 4$. As discussed in Section 3, we set the CLWE distribution in the DWT domain, which does not affect the choice of γ . We set $\beta = 0.01$ arbitrarily. This choice creates a series of “gaussian pancakes” with spacing 0.25 in the latent space. Since the image sampling and inversion processes add significant noise, this may not be usable in practice.

We can consider smaller parameter values for γ using more recent theoretical results. In [19], it is suggested that if the subexponential hardness of LWE can be assumed, then $\gamma = (\log n)^{\frac{1}{2} + \delta} \log \log n$ should be sufficient, for arbitrarily small $\delta > 0$. To evaluate this choice, we performed a statistical simulation of the covariance attack described in [4], as a representative of the best known direct attacks on CLWE. In this attack, the adversary computes the covariance matrix of a large set of samples, computes the eigenvalues, and finds the maximum difference with $1/2\pi$, see Algorithm 2 for an explicit description. To complete the attack, the adversary checks if this score is greater than $\gamma^2 \exp(-\pi(\beta^2 + \gamma^2))$.

5. Note that quality is determined by oracles with no access to keys.

Algorithm 2: Covariance method to determine if samples are from a CLWE distribution or standard normal.

Input: Samples $A \in \mathbb{R}^{m \times n}$

Output: Covariance score

- 1 $\Sigma_m \leftarrow \frac{1}{2\pi m} A^T A$;
 - 2 $\mu_1, \dots, \mu_n \leftarrow \text{eigenvalues}(\Sigma_m)$;
 - 3 **return** $\max_{i \in [n]} |\mu_i - \frac{1}{2\pi}|$;
-

In our statistical simulation, we generated 10,000 samples in \mathbb{R}^n from the standard normal distribution, along with 10,000 samples from the CLWE distribution for varying values of γ , all for several values of n , and plot the scores for both along with the threshold for the attack in Figure 9. From this we make the following observations:

- 1) The attack is generally successful for $\gamma < 1$.
- 2) The range of effective γ does not increase with n .
- 3) The threshold given in [4] is only useful in a small range, otherwise, it is more useful to characterise the expected score for a normal distribution.
- 4) The value of n only seems to affect the number of samples needed to eliminate the hypothesis of a normal distribution, but does not affect the value of γ needed to prevent the attack.

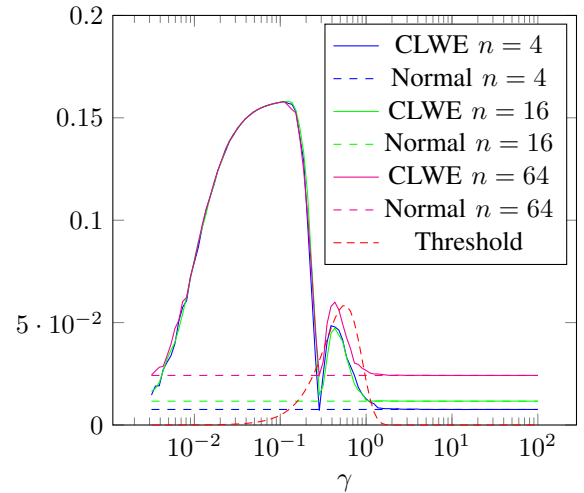


Figure 9: Covariance attack scores from a statistical simulation of 10,000 points.

From this we conclude that setting $\gamma \geq 1$ with larger dimensions may be more practical, in particular since in our setting the number of samples per image is reduced with larger n while also increasing the number of samples needed for the attack to be successful. This matches the limit from [19].

With $n = 4$ setting $\gamma \geq 4, \beta = 0.01$ provides theoretical security, while $n = 64, \gamma \geq 1, \beta = 0.01$

should provide security against practical attacks.

We stress that our proposed parameters are close to, but not exactly equal to those needed in the tightest theoretical reductions of CLWE hardness given in prior works. Further research on tighter reductions and the concrete parameters to use in practice is important future work. For this reason we provide theoretical proofs of security that apply to any choice of γ and β , but use the parameters from this section in order to show a proof-of-concept.

6.2. Evaluation Setup

We perform our evaluation on state-of-the-art text to image open sourced diffusion models, specifically, Stable Diffusion version 2.1. We generate 512×512 images starting with latent embeddings of size $4 \times 64 \times 64$ in 50 steps. For inverting the diffusion process we evaluate both the DDIM process of [17] and the enhanced process of [16].

Datasets. We use two standard benchmark datasets: Stable Diffusion Prompts (SDP)⁶, and COCO [20]. We generate an image without a watermark and for each watermarking technique using the same prompt and initial seed, for each of the first 1,000 prompts in each dataset.

Baselines. TREE RING and GAUSSIAN SHADING are the two state-of-the-art pre-processing based watermarking techniques that claim some level of undetectability unlike the post-processing based methods which are known to be detectable [1]. We use these two methods as our baselines. We use the “ring” pattern for TREE RING, and the standard GAUSSIAN SHADING method, but note that we fixed the key and nonce for all images. The original code for GAUSSIAN SHADING generated a fresh key and nonce for each image, which is not practical since the recovery process would not have access to the key and nonce for a specific image.

Evaluation Metrics. We use Frechet Inception Distance (FID) [21] to measure the quality of generated images. FID measures the difference in the embeddings between two images using the Inception model, which is a heuristic for how similar they are. Measuring the FID between the watermarked images and their unwatermarked counterparts gives a sense of the quality degradation of the watermarking scheme, i.e. a lower FID implies better quality images.

All of the watermarking schemes produces a score indicative of the likelihood of the watermark being present in the image. Thus, the performance of the watermarking scheme depends on choosing a threshold for this score. By plotting the true positive rate (TPR) vs false positive rate (FPR) curve for varying thresholds we obtain the Receiver Operating Characteristic (ROC) curve, a commonly used method for evaluating the performance of binary classifiers. The area under the ROC curve (AUC) is a metric that summarizes the performance of the classifier. A score of

6. <https://huggingface.co/datasets/Gustavosta/Stable-Diffusion-Prompts>

n	γ	Inv Method	COCO AUC	SDP AUC
64	1	DDIM	0.958	0.947
4	4	Enh Inv	0.990	0.997

TABLE 1: AUC scores for CLUE-MARK recovery.

1 indicates perfect performance, while a score of 0.5 indicates performance no better than random. Thus we use the AUC score to evaluate the performance of the watermarking schemes.

System Specification. We ran our experiments on an Intel Xeon Gold 6230 processor with 256 GB of RAM and 8 Nvidia RTX 2080 Ti GPUs with 11 GB of memory each, running CUDA 11.8 and Nvidia drivers 520.56.06, except for the experiments using the enhanced inverse DPM process, for which we used an AMD Ryzen 3970X processor with 98 GB of RAM and 2 Nvidia RTX 2080 Ti GPUs with 24 GB of memory each, running CUDA 11.4 and Nvidia drivers 470.256.02.

6.3. RQ2. Watermark Recovery

We answer how sound and complete CLUE-MARK’s recovery strategy is by producing a watermarked and unwatermarked image for each of the 1,000 prompts. As discussed in Section 6.1 we set $\gamma = 1, \beta = 0.01$ with a block size of $4 \times 4 \times 4$ and apply the watermark in the DWT domain. We then apply CLUE-MARK’s recovery strategy to all the images and compare the results. We find that for both datasets, CLUE-MARK is able to distinguish between watermarked and unwatermarked images with high accuracy. See Table 1 for the AUC scores. For comparison, the baseline techniques produced AUC scores of 1.0 for the same conditions.

We also evaluated the theoretical secure parameters $n = 4, \gamma = 4, \beta = 0.01$ and found that with DDIM the watermark could not be recovered consistently, as the noise introduced simply swamped the CLWE distribution. By using the enhanced inverse DPM process [16] we were able to recover the watermark with high accuracy, but the process took considerably longer (DDIM with 16-bit numbers took ~ 2.2 s per image, while the enhanced order 1 solver using 32-bit numbers took ~ 97 s on average to process an image). Thus, we were only able to analyse 100 images. As shown in Table 1, the enhanced process is able to recover the watermark with an AUC > 0.99 in both datasets.

Using the practical parameters, CLUE-MARK’s detector has high soundness and completeness (AUC scores > 0.9) in unperturbed images across all of our evaluated settings using standard DDIM.

Using the theoretical secure parameters and the enhanced inverse DPM process, CLUE-MARK’s detector has high soundness and completeness (AUC scores > 0.99) in unperturbed images.

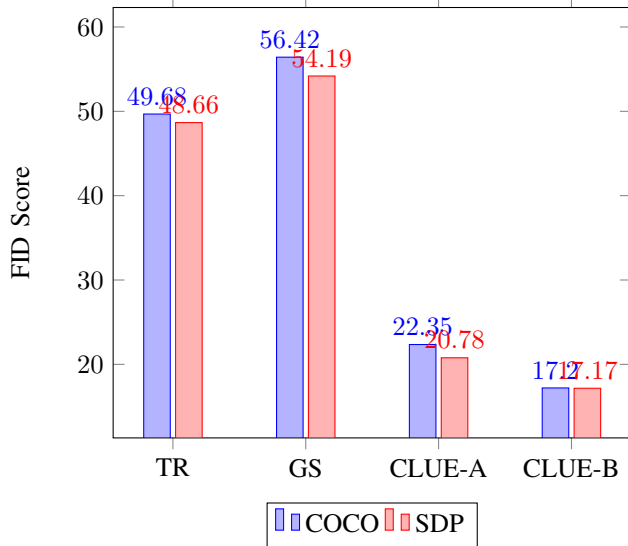


Figure 10: Image quality as measured by FID to unwatermarked images. TR refers to Tree Ring, GS to Gaussian Shading, CLUE-A to CLUE-MARK with practical parameters, $n = 64, \gamma = 1, \beta = 0.01$, and CLUE-B to CLUE-MARK with theoretical parameters, $n = 4, \gamma = 4, \beta = 0.01$.

6.4. RQ3. Image Quality

As can be seen in Figure 10, CLUE-MARK in either configuration generates images with the closest quality to the non-watermarked images for both datasets, while GAUSSIAN SHADING and TREE RING produces an FID distance two to three times greater (worse) than CLUE-MARK.

The degradation in quality of the images indicates that both the baselines are not undetectable, especially when many watermarked images are analyzed at once for detectability. This is expected for TREE RING since it does not embed provably undetectable watermarks. It is also expected for GAUSSIAN SHADING as it only proves undetectability for a single image. We explain this in detail in our discussion regarding GAUSSIAN SHADING in Section 6.5.

CLUE-MARK generates images with similar quality to non-watermarked images and up to $3\times$ higher quality images than the baselines.

6.5. RQ4. Resilience to Steganographic Attacks

A steganographic attack attempts to remove the watermark from marked images by averaging the difference between the watermarked and unwatermarked images over many samples. In order to compare with prior work and confirm the theory behind our construction, we reproduced the results from [2] using 1,000 pairs of watermarked and unwatermarked images generated for each watermarking method, and average the difference between the images. As can be seen in the examples in Figure 11, there are

Watermark	COCO	SDP
TREE RING	0.616	0.457
GAUSSIAN SHADING	0.458	0.569
CLUE-MARK A	0.933	0.937
CLUE-MARK B	0.998	0.989

TABLE 2: AUC scores after steganographic attack.

obvious patterns in the averages from TREE RING and GAUSSIAN SHADING, but CLUE-MARK produces a nearly blank image. We then subtract this average from the watermarked images and attempt to recover the watermark. As shown in Table 2, the attack successfully removes the TREE RING and GAUSSIAN SHADING watermarks, but is unable to remove the CLUE-MARK watermark. We note that the resulting watermark-removed images for TREE RING are of similar quality, but for GAUSSIAN SHADING suffer some degradation. We expect that a more sophisticated attack could remove the GAUSSIAN SHADING watermark without degrading the image.

CLUE-MARK is robust to standard steganographic attacks unlike the baselines whose watermark can be detected and removed.

6.6. RQ5. Robustness to Benign Transformations

We evaluate the robustness of CLUE-MARK and the baseline techniques under different non-adversarial post-processing techniques. Specifically, we apply JPEG compression, brightness, Gaussian blur, cropping, and rotations to the watermarked images and measure recovery performance. Our results are shown in Figure 12. For comparison, the baselines all produced AUC scores at or near 1.0 for all conditions. We observe that CLUE-MARK somewhat robust to JPEG compression and brightness changes, but not to the other perturbations. Thus CLUE-MARK is robust to minor perturbation, but any significant modifications make the watermark unrecoverable. We leave improving the robustness of CLUE-MARK to accommodate cropping and rotation to future work.

CLUE-MARK is robust to minor perturbations such as JPEG compression and brightness but not robust to larger perturbations.

7. Related Work

Watermarking images has been extensively studied since the 1990s [22]. Early research primarily focused on watermarking individual images, while more recent advancements target AI-generated images. Unlike traditional images, AI-generated content allows watermarking at various stages of the generation pipeline, including altering training data or fine-tuning models to embed watermarks.

Individual Images. Post-processing techniques are commonly applied to individual images, embedding watermarks



Figure 11: Steganographic attack examples.

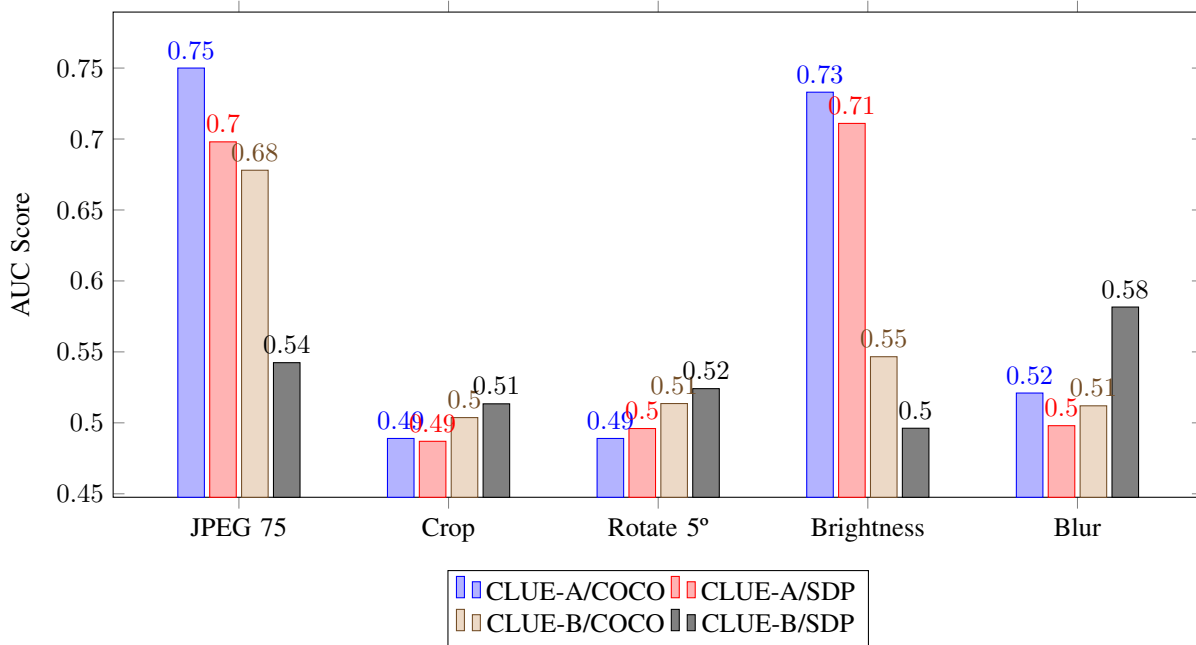


Figure 12: Robustness to common perturbations as measured by RoC AUC.

by modifying images after creation. Classical methods operate in either the spatial [22], [23] or frequency domain [15], [24], [25], [26], [27]. Spatial domain techniques modify pixel intensities, often by altering the least significant bits of selected pixels. While efficient, these techniques lack robustness against simple transformations like brightness adjustments or JPEG compression. In contrast, frequency domain methods embed watermarks by altering an image’s frequency coefficients after applying a transformation such as the Discrete Cosine Transform (DCT) or Discrete Wavelet Transform (DWT). These approaches offer greater robustness to perturbations, while ensuring that the watermark remains imperceptible, often measured by peak signal-to-noise ratio (PSNR).

More recently, many deep learning-based techniques have been introduced in order to enhance robustness and quality [28], [29], [30], [31], [32]. These techniques typically leverage encoder-decoder neural architectures, where the encoder embeds a message into an image, and the decoder recovers the message. The models are trained to minimize differences between the watermarked and original images for even an adversarial classifier, while ensuring message recovery even in the presence of noise. Various architectures, noise injection strategies, and training objectives have been explored to achieve robustness against diverse transformations.

However, existing post-processing methods lack provable guarantees of undetectability and may degrade image quality [1], [33]. Additionally, using the same watermark across multiple images can expose vulnerabilities to steganographic attacks, allowing the watermark to be extracted [2].

Generative Models. Generative models like Generative Adversarial Networks (GANs) and Latent Diffusion Models have become standard for producing high-fidelity, ultra-realistic images. When traditional watermarking methods are applied to AI-generated images, they often reduce visual quality [33], which is clearly undesirable.

Recent research addresses this issue by embedding watermarks directly within the generative process [1], [3], [33], [34], [35], [36]. One approach involves training parts of the model to embed messages during generation, allowing extraction via a pre-trained decoder [33], [34], [35], [36]. However, these techniques require multiple training rounds, which is computationally expensive, especially as the size of state-of-the-art models continues to grow. While these methods claim improved image quality over post-processing techniques, they rely on ad-hoc metrics like PSNR and are significantly more resource-intensive.

Recent advances in watermarking latent diffusion model images propose modifying only the input latent vectors, offering computational efficiency without altering model parameters [1], [3]. Diffusion models then generate images normally, unaware of the modification to the latents. The watermarks are detected by reversing the diffusion process and examining latent vector. Techniques such as Tree Ring [1] and Gaussian Shading [3] claim state-of-the-art performance in both visual quality, in the sense that they

are imperceptible to human observers, and robustness, in the sense that after common image perturbations the watermark can still be recovered. However, none of these techniques provide provable undetectability; the watermarks can still be identified, removed, or forged by steganographic attacks [2].

Our work advances these approaches by introducing a watermarking scheme that is provably undetectable and unforgeable. Our tool, CLUE-MARK, achieves optimal image quality in latent diffusion model outputs yet watermarks cannot be identified or forged without the secret key. Uniquely, it leverages cryptographically hard lattice problems, specifically the CLWE (Continuous Learning with Errors) problem, to embed watermarks. This is a novel application in the context of generative models, as prior research using such cryptographic techniques has focused on implanting undetectable backdoors in random Fourier feature-based models for classification tasks [37].

8. Conclusions and Future Work

In this work we introduced CLUE-MARK, the first provably undetectable watermarking scheme for diffusion model generated images, leveraging the cryptographic hardness of the Continuous Learning With Errors (CLWE) problem. We first defined formally what it means for a watermark scheme to be undetectable, and then described how CLUE-MARK works. We then proved that CLUE-MARK is undetectable under the hCLWE assumption. Finally, we evaluated empirically the performance of CLUE-MARK on common diffusion models and datasets, showing that it is usable in practice, produces images with much higher fidelity to the original unwatermarked images than existing techniques, and cannot be detected by steganographic techniques. CLUE-MARK is robust to some common perturbations, such as JPEG compression and brightness changes, but not to cropping, rotation, and blur.

Future work may consider improving the robustness of CLUE-MARK to perturbations. Also, the concrete parameters for CLWE are not yet well studied, and it is possible that better parameters could improve the performance of CLUE-MARK while maintaining undetectability. Finally, the technique used for inverting the model to obtain the estimate of the original latent vector is the current bottleneck in recovering the watermark in terms of both quality and speed. Improvements to the inversion method would significantly improve the performance of CLUE-MARK.

Acknowledgments

We are thankful to thank Ivica Nikolic, Wenjie Qu, and Rohit Chatterjee for their helpful feedback on previous drafts. This research is supported by the research funds of the Crystal Centre at National University of Singapore, Cisco University Research Program Fund, a corporate advised fund of Silicon Valley Community Foundation. All opinions expressed in the work are those of the authors.

References

- [1] Y. Wen, J. Kirchenbauer, J. Geiping, and T. Goldstein, "Tree-ring watermarks: Fingerprints for diffusion images that are invisible and robust," 2023. [Online]. Available: <https://arxiv.org/abs/2305.20030>
- [2] P. Yang, H. Ci, Y. Song, and M. Z. Shou, "Steganalysis on digital watermarking: Is your defense truly impervious?" 2024. [Online]. Available: <https://arxiv.org/abs/2406.09026>
- [3] Z. Yang, K. Zeng, K. Chen, H. Fang, W. Zhang, and N. Yu, "Gaussian shading: Provable performance-lossless image watermarking for diffusion models," 2024. [Online]. Available: <https://arxiv.org/abs/2404.04956>
- [4] J. Bruna, O. Regev, M. J. Song, and Y. Tang, "Continuous lwe," 2020. [Online]. Available: <https://arxiv.org/abs/2005.09595>
- [5] D. Podell, Z. English, K. Lacey, A. Blattmann, T. Dockhorn, J. Müller, J. Penna, and R. Rombach, "Sdxl: Improving latent diffusion models for high-resolution image synthesis," *arXiv preprint arXiv:2307.01952*, 2023.
- [6] R. Rombach, A. Blattmann, D. Lorenz, P. Esser, and B. Ommer, "High-resolution image synthesis with latent diffusion models," in *CVPR*, 2022.
- [7] L. Yang, Z. Zhang, Y. Song, S. Hong, R. Xu, Y. Zhao, W. Zhang, B. Cui, and M.-H. Yang, "Diffusion models: A comprehensive survey of methods and applications," *ACM Computing Surveys*, 2023.
- [8] N. Henry and R. Umbach, "Sextortion: Prevalence and correlates in 10 countries," *Computers in Human Behavior*, 2024.
- [9] F. Explainers, "How deepfake romance scammers stole 46 million from men in india, china, singapore," 2024, <https://www.firstpost.com/explainers/how-deepfake-romance-scammers-stole-46-million-from-men-in-india-china-singapore-13825760.html>.
- [10] N. Robins-Early, "How did donald trump end up posting taylor swift deepfakes?" 2024. [Online]. Available: <https://www.theguardian.com/technology/article/2024/aug/24/trump-taylor-swift-deepfakes-ai>
- [11] O. of Public Affairs, "Department of commerce announces new actions to implement president biden's executive order on ai," 2024, <https://www.commerce.gov/news/press-releases/2024/04/department-commerce-announces-new-actions-implement-president-bidens>.
- [12] B. Diane and H. Krystal, "Openai, google, others pledge to watermark ai content for safety, white house says," 2024, <https://www.reuters.com/technology/openai-google-others-pledge-watermark-ai-content-safety-white-house-2023-07-21/>.
- [13] T. Madiaga, "Generative ai and watermarking," 2023, [https://www.europarl.europa.eu/RegData/etudes/BRIE/2023/757583/EPRS_BRI\(2023\)757583_EN.pdf](https://www.europarl.europa.eu/RegData/etudes/BRIE/2023/757583/EPRS_BRI(2023)757583_EN.pdf).
- [14] D. Seetharaman and M. Barnum, "There's a tool to catch students cheating with chatgpt. openai hasn't released it." *The Wall Street Journal*, 2023. [Online]. Available: <https://www.wsj.com/tech/ai/openai-tool-chatgpt-cheating-writing-135b755a>
- [15] A. Al-Haj, "Combined dwt-dct digital image watermarking," *Journal of computer science*, 2007.
- [16] S. Hong, K. Lee, S. Y. Jeon, H. Bae, and S. Y. Chun, "On exact inversion of dpm-solvers," in *CVPR*, 2024.
- [17] J. Song, C. Meng, and S. Ermon, "Denoising diffusion implicit models," *arXiv preprint arXiv:2010.02502*, 2020.
- [18] Q. Pang, S. Hu, W. Zheng, and V. Smith, "No free lunch in llm watermarking: Trade-offs in watermarking design choices," 2024. [Online]. Available: <https://arxiv.org/abs/2402.16187>
- [19] A. Gupte, N. Vafa, and V. Vaikuntanathan, "Continuous lwe is as hard as lwe & applications to learning gaussian mixtures," in *2022 IEEE 63rd Annual Symposium on Foundations of Computer Science (FOCS)*, 2022, pp. 1162–1173.
- [20] T.-Y. Lin, M. Maire, S. Belongie, J. Hays, P. Perona, D. Ramanan, P. Dollár, and C. L. Zitnick, "Microsoft coco: Common objects in context," in *ECCV*, 2014.
- [21] M. Heusel, H. Ramsauer, T. Unterthiner, B. Nessler, and S. Hochreiter, "Gans trained by a two time-scale update rule converge to a local nash equilibrium," *NeurIPS*, 2017.
- [22] R. G. Van Schyndel, A. Z. Tirkel, and C. F. Osborne, "A digital watermark," in *IEEE Proceedings of 1st international conference on image processing*, 1994.
- [23] M.-J. Tsai, K.-Y. Yu, and Y.-Z. Chen, "Joint wavelet and spatial transformation for digital watermarking," *IEEE Transactions on Consumer Electronics*, 2000.
- [24] H. Guo and N. D. Georganas, "Digital image watermarking for joint ownership," in *Proceedings of the tenth ACM international conference on Multimedia*, 2002.
- [25] M. Hamidi, M. E. Haziti, H. Cherifi, and M. E. Hassouni, "Hybrid blind robust image watermarking technique based on dft-dct and arnold transform," *Multimedia Tools and Applications*, 2018.
- [26] D. Kundur and D. Hatzinakos, "A robust digital image watermarking method using wavelet-based fusion," in *IEEE Proceedings of International Conference on Image Processing*, 1997.
- [27] S. Lee, C. D. Yoo, and T. Kalker, "Reversible image watermarking based on integer-to-integer wavelet transform," *IEEE Transactions on information forensics and security*, 2007.
- [28] Z. Jia, H. Fang, and W. Zhang, "Mbrs: Enhancing robustness of dnn-based watermarking by mini-batch of real and simulated jpeg compression," in *Proceedings of the 29th ACM international conference on multimedia*, 2021.
- [29] M. Tancik, B. Mildenhall, and R. Ng, "Stegastamp: Invisible hyperlinks in physical photographs," in *Proceedings of the IEEE/CVF conference on computer vision and pattern recognition*, 2020.
- [30] J. Zhu, "Hidden: hiding data with deep networks," *arXiv preprint arXiv:1807.09937*, 2018.
- [31] Y. Liu, M. Guo, J. Zhang, Y. Zhu, and X. Xie, "A novel two-stage separable deep learning framework for practical blind watermarking," in *Proceedings of the 27th ACM International conference on multimedia*, 2019.
- [32] M. Ahmadi, A. Norouzi, N. Karimi, S. Samavi, and A. Emami, "Redmark: Framework for residual diffusion watermarking based on deep networks," *Expert Systems with Applications*, 2020.
- [33] P. Fernandez, G. Couairon, H. Jégou, M. Douze, and T. Furon, "The stable signature: Rooting watermarks in latent diffusion models," in *Proceedings of the IEEE/CVF International Conference on Computer Vision*, 2023.
- [34] N. Yu, V. Skripniuk, D. Chen, L. Davis, and M. Fritz, "Responsible disclosure of generative models using scalable fingerprinting," *ICLR*, 2022.
- [35] N. Yu, V. Skripniuk, S. Abdelnabi, and M. Fritz, "Artificial fingerprinting for generative models: Rooting deepfake attribution in training data," in *ICCV*, 2021.
- [36] N. Lukas and F. Kerschbaum, "{PTW}: Pivotal tuning watermarking for {Pre-Trained} image generators," in *USENIX Security*, 2023.
- [37] S. Goldwasser, M. P. Kim, V. Vaikuntanathan, and O. Zamir, "Planting undetectable backdoors in machine learning models," in *2022 IEEE 63rd Annual Symposium on Foundations of Computer Science (FOCS)*, 2022.